

Accepted Manuscript

Multiresolution wavelet transform based feature extraction and ECG classification to detect cardiac abnormalities

Santanu Sahoo, Bhupen Kanungo, Suresh Behera, Sukanta Sabut

PII: S0263-2241(17)30297-X
DOI: <http://dx.doi.org/10.1016/j.measurement.2017.05.022>
Reference: MEASUR 4748

To appear in: *Measurement*

Received Date: 27 November 2015
Revised Date: 3 April 2017
Accepted Date: 9 May 2017

Please cite this article as: S. Sahoo, B. Kanungo, S. Behera, S. Sabut, Multiresolution wavelet transform based feature extraction and ECG classification to detect cardiac abnormalities, *Measurement* (2017), doi: <http://dx.doi.org/10.1016/j.measurement.2017.05.022>

This is a PDF file of an unedited manuscript that has been accepted for publication. As a service to our customers we are providing this early version of the manuscript. The manuscript will undergo copyediting, typesetting, and review of the resulting proof before it is published in its final form. Please note that during the production process errors may be discovered which could affect the content, and all legal disclaimers that apply to the journal pertain.



Multiresolution wavelet transform based feature extraction and ECG classification to detect cardiac abnormalities

Santanu Sahoo^a, Bhupen Kanungo^a, Suresh Behera^b, Sukanta Sabut^{c*}

^aDept. of Electronics & Communication Engineering, Institute of Technical Education & Research, SOA University, Bhubaneswar, Odisha, INDIA

^bDept. of Cardiology, IMS & SUM Hospital, SOA University, Bhubaneswar, Odisha, INDIA

^cDept. of Electronics & Instrumentation Engineering, Institute of Technical Education & Research, SOA University, Bhubaneswar, Odisha, INDIA

ABSTRACT

Analysis of electrocardiogram (ECG) signal provides valuable information about the heart conditions of the patient to the clinicians. The wavelet transform is an effective tool for extracting discriminative features in ECG signal classification for automatic diagnosis of cardiac arrhythmia. In this paper we proposed an improved algorithm to detect QRS complex features based on the multiresolution wavelet transform to classify four types of ECG beats. Extracted features are used for classifying cardiac abnormalities: normal (N), left bundle branch block (LBBB), right bundle branch block (RBBB), Paced beats (P) using neural network (NN) and support vector machines (SVM) classifier. The performance of the method is evaluated in terms of sensitivity, specificity, accuracy for 48 recorded ECG signals obtained from the MIT-BIH arrhythmia database. The proposed process achieved high detection performance with less error rate of 0.42% in detecting QRS complex. The classifier confirmed the superiority with an average accuracy of 96.67% and 98.39% in NN and SVM respectively. The classification accuracy of SVM approach proves superior for the proposed method to that of the NN classifier with extracted parameter in detecting ECG arrhythmia beats.

Keywords: Electrocardiogram; wavelet; QRS complex; features; neural networks; SVM.

1. Introduction

Heart disease and heart stroke is a major threat to human life. Every year 17.1 million lives are claimed globally out of which 82% cases are from developing countries [1]. In a country like India, the coronary heart disease, and diabetes are responsible for 1.3 to 4.6 million deaths per year with an annual incidence of 491,600 to 1.8 million [2]. Nearly 80% of

sudden cardiac death are caused by ventricular arrhythmias which is one of the most common cardiac arrhythmia condition that causes irregular heartbeats [3-5]. The identification of risk factor of cardiac arrest could be improved with early detection of arrhythmia conditions from the analysis of ECG signals. The peaks and valleys of ECG signal are labelled by the waves P, Q, R, S, and T that represent the activation of the atria and ventricular repolarization [6-7]. The different interferences like the baseline wanders, power line interference and physiological artefacts corrupt the ECG signal [8].

Several methods have been reported for eliminating these noises from ECG signal. Some of the most used methods are mathematical morphology [9], empirical mode decomposition [10], adaptive filtering [11], band pass filter [12], and weighted averaging filter [13], principal component analysis [14] and independent component analysis [15]. The features of ECG signal can be extracted in time domain [16], frequency domain [17], and can be represented as statistical measures [18]. The energy of heart beats is mainly located in the QRS complex of the ECG waveform and accurate detection of this complex is a vital part of ECG analysis [19]. The filtering and smoothing techniques are applied in pre-processing stage to attenuate P and T waves as well as noise [20]. The computation of QRS duration starts with detecting the QRS onset and offset points which starts from the R-peaks. Locating proper fiducial point could determine the accurate QRS complex for further analysis of ECG signal [21, 22].

Numerous algorithms are used for QRS detection based on digital filters and non-linear transforms in order to extract the feature components [23, 24]. A multi-scale QRS detector using discrete wavelet transformation (DWT) have been used for finding the modulus maxima. DWT has been used in many applications in signal processing domain. DWT decomposes a signal into different coarseness with coefficients that represent the sufficient information of the original signal as the filtered signal in the sub-bands [25, 26]. The QRS complex, P and T-wave can be detected with detection rate of 99.8% in presence of baseline drift and noise by the use of multiscale feature of WT's, [27]. A Dyadic Wavelet based has been proposed by Martinez et al., to find both positive maximum and negative minimum peaks [28]. An accuracy of 97% has been obtained with the use of multiresolution wavelet transform to detect and evaluate QRS complex, P and T waves [29]. The concept of dominant rescaled wavelet coefficients (DRWC) was used to magnify QRS complex and to reduce the effects of other peaks. The classification result based on morphology to detect QRS has shown an average sensitivity of 99.91% and a positive predictivity 99.72% [30]. In a recent work, the multiresolution WT with adaptive thresholding was used detected the peaks and

waves of ECG signals with sensitivity and positive predictivity of 99.8% and 99.6% for MIT BIH Arrhythmia database and 99.84% and 99.98% for PTB ECG database [31]. The multiresolution wavelet analysis based on power spectrum of decomposition signals is used for selecting detail coefficient corresponding to parameters λ_1 and λ_2 frequency band of the QRS complex. The evaluated result shows the good detection performance with global sensitivity of 99.87%, positive predictivity of 99.79% with an error rate of 0.34% [32]. This work focuses mainly on cardiac arrhythmia detection and classification. A large number of approaches have been proposed in the literature for the classification of cardiac arrhythmia. Some of these approaches being linear discriminants [45], artificial neural networks (ANNs) [8] and support vector machines (SVMs) [47]. A robust classifier called optimum-path forest (OPF) based on supervised graph pattern recognition technique has been employed for fast and accurate classification of cardiac beats [49].

The morphological changes occurs in ECG signal due to pathological conditions therefore developing a robust algorithm for accurate detection of the QRS complex and R-peaks is a challenging task. In this paper we proposed an improved algorithm to detect QRS complex structure and R-peaks with an innovative viewpoint using the multiresolution wavelet transform with amplitude thresholding. We aim to evaluate the effectiveness of the proposed method for detecting the cardiac arrhythmias i.e. normal, LBBBs, RBBBs and paced beats using neural network (NN) and SVM classifiers. The informative features were extracted from the processed signal and used in classifiers to classify the ECG beat types and the obtained results were compared with other reported results.

2. Methodology

The ECG signals were taken from MIT-BIH arrhythmia database with a sampling frequency of 360 Hz are converted to matlab format (.mat) [22]. It contains 48 records of 30 minutes duration ECG signals with 11-bit resolution over a 10 mV range. The block diagram of the proposed QRS complex detection algorithm for ECG signal is shown in Fig.1. It includes digital filtering, QRS detection, R-peak detection, on and off peaks and morphological parameter extraction. The algorithm was implemented using MATLAB version 2012, and it was tested on the ECG signals taken from the first channel (MLII). The average processing time required for performing our method on each 30 min ECG data is approximately 1.33s.

2.1. Multiresolution wavelet transform

Many potential transform like Hilbert transform, short time Fourier transform (STFT), and wavelet transform are widely used for non-stationary biomedical signals. Multiresolution wavelet transform provides the time-frequency representation of the signal with time localization of spectral components [29]. The low pass and the high pass filters of DWT have a property that they can be obtained as the weighted sum of the scaled (dilated) and shifted version of the scaling function itself. DWT function can be derived as

$$\phi_{m,n}(t) = \frac{1}{\sqrt{a^m}} \phi\left(\frac{t-nba^m}{a^m}\right) \quad (1)$$

where ϕ is the wavelet function, m , and n are the integers which control the wavelet dilation and translation respectively, a is the specific fixed dilation step parameter which is greater than 1 ($=2$ for this case) and b is the location parameter which is greater than 0 ($=1$ for this case). The power of two logarithmic scaling of both the dilation and translation steps is known as the grid arrangement and substituting the grid values of a and b , equation (1) can be written as $\phi_{m,n}(t) = 2^{-\frac{m}{2}} \phi(2^{-m}t - n)$

(2)

Using dyadic grid given in equation (2) the DWT can be expressed as

$$T_{m,n} = \int_{-\infty}^{+\infty} x(t) \phi_{m,n}(t) dt \quad (3)$$

where $T_{m,n}$ is the wavelet coefficients, m , and n are the scale and location respectively.

The relation between impulse response of high pass and low pass filters of DWT is

$$g(L - n - 1) = (-1)^n h(n) \quad (4)$$

Where $g(n)$ and $h(n)$ are the high pass and low pass filters. The filter length is L . The filtering and sub-sampling operation can be expressed by:

$$y_{high}(k) = \sum_n x(n) g(-n + 2k) \quad (5)$$

$$\text{And } y_{low}(k) = \sum_n x(n) h(-n + 2k) \quad (6)$$

because of orthonormal bases the half band filters are easily reconstruct by

$$x(n) = \sum_{-\infty}^{+\infty} [y_{high}(k) \cdot g(-n + 2k)] + [y_{low}(k) \cdot h(-n + 2k)] \quad (7)$$

if the filters are not ideal half band then perfect reconstruction is not possible.

2.2. Pre-processing

The selection of a particular wavelet function that matches closely to the morphology of the signal under consideration is the most important factor for signal decomposition [23]. In the pre-processing stage, the noises have been eliminated by decomposing non-informative frequency components with multiresolution wavelet transform using Daubechies (db6) to enhance the important morphology of the QRS complex of ECG signal. The signal is enhanced by eliminating noise with corresponding detail coefficients from high frequency ranges at D_1 , D_2 and low frequency ranges at A_{10} .

2.3. R-peak detection

The maximum amplitude of de-noised ECG signals is considered as R-wave positions. Fig. 2 illustrates the flowchart of R-wave detection algorithm, which is summarized as QRS complex can be obtained by taking the sum of maximum informative decomposed wavelets from the DWT i.e. D_3 , D_4 and D_5 . A pragmatic threshold of 15% of the maximum amplitude of $(D_3+D_4+D_5)$ was selected to obtain a good localization of the used windows around QRS region. Each beat of QRS complex is assigned with a window of 160 ms and a searching process is initiated around the QRS beats which determine the greater amplitude than the predefined threshold level. The maximum amplitude of the de-noised ECG signal determines the R-peak positions of the predefined window. The refractory period of 200 ms is taken between two consecutives searches in which ventricular depolarisation cannot occur. The detected maximum peaks is considered as R-peaks and stored in an array of R_Loc

2.4. QRS complex detection

Based on the power spectrum of QRS band energy, the remaining detail coefficients are used for the detection of QRS complex positions. A combination of the three sets of detail coefficients D_3 , D_4 and D_5 is selected based on frequency ranges. To find the beginning of the window with a specific width (160 ms), a threshold level 15% of max. $(D_3+D_4+D_5)$ is taken for extraction of features. A sliding window of 200 ms is used to detect the R peak position in each window location by locating the fiducial position.

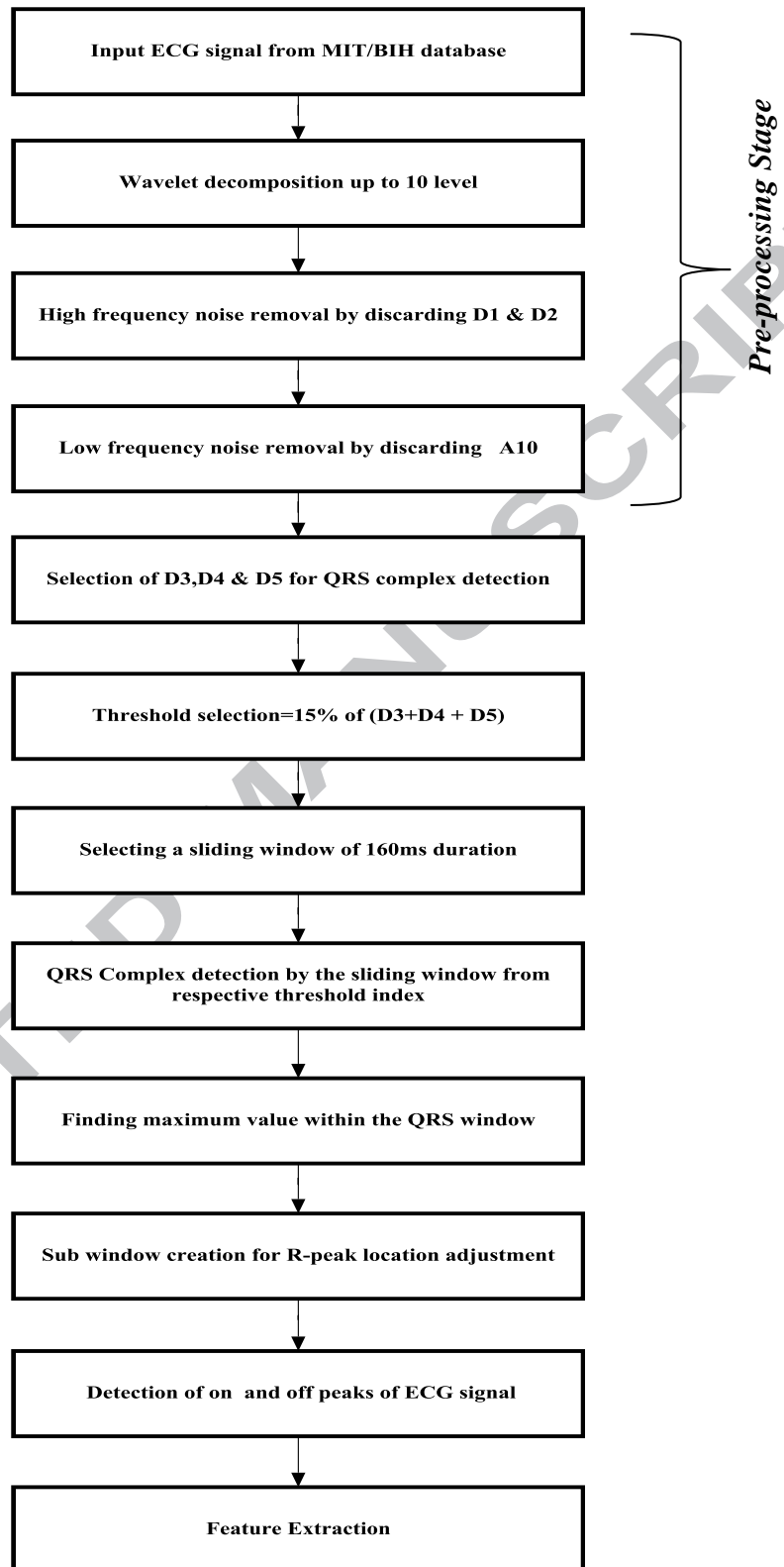


Fig.1. Block diagram of the proposed QRS complex detection algorithm

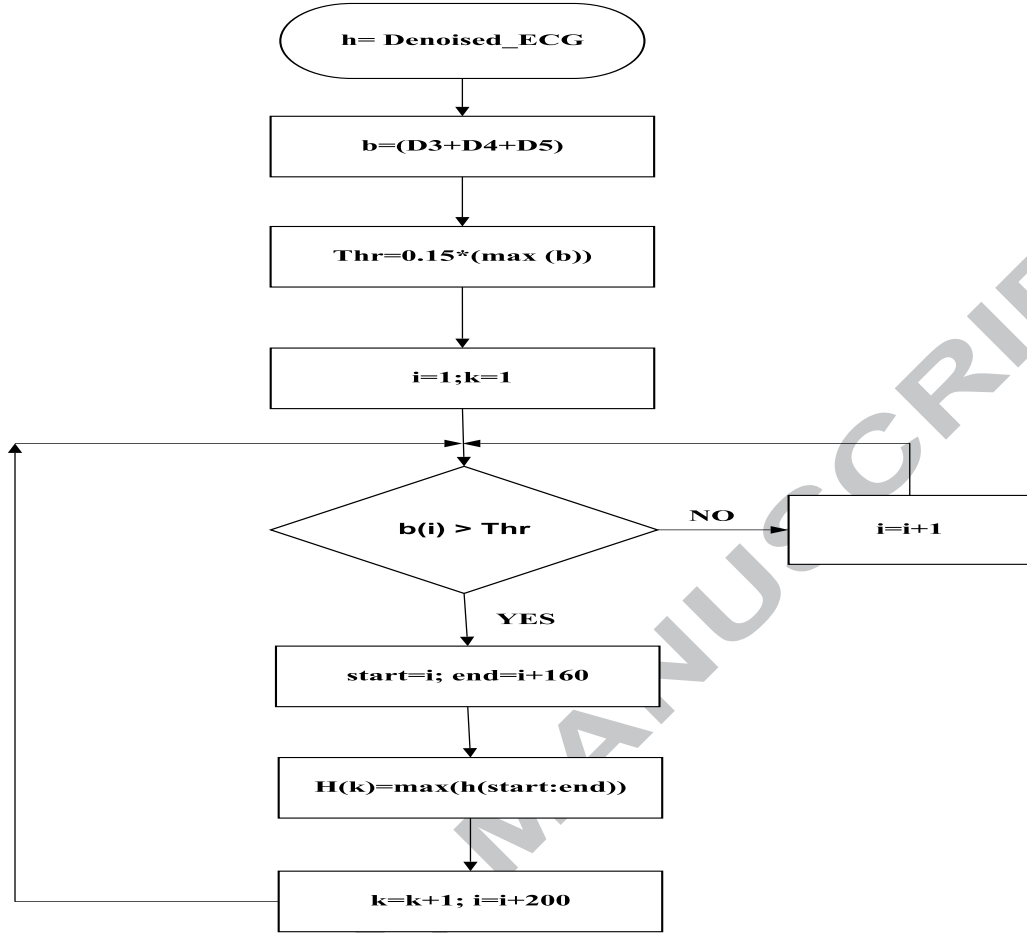


Fig. 2. Flow diagram for R-peak detection

2.5. Classification methods

2.5.1. Multilayer Perceptron (MLP) neural network

Neural networks classifier is most widely used in ECG signal analysis [8]. The Multilayer Perception (MLP) is commonly implemented neural network topologies. MLPs are trained with the back propagation algorithm which propagates the errors through the network and allows adaptation of the hidden nodes. The function can be expressed as:

$$y = \sum_{i=1}^d x_i w_{ij} \quad (8)$$

where x_i are the set of inputs $x = [x_1, x_2, x_3 \dots \dots x_n]^T$ and w_{ij} are the set of weights $w = [w_1, w_2, w_3, \dots \dots w_n]^T$.

The error is calculated as $e_i(n) = d_i(n) - y_i(n)$ using gradient descent learning, each weight in the network is adapted by correcting the present value of the input and error at the weight i.e., $w_{ij}(n+1) = w_{ij}(n) + \eta \delta_i(n) x_j(n)$, where η is the learning rate. The experimental architecture of MLP is designed with eight input features in the input layer,

single hidden layer and four classes in the output layers to classify the ECG beats, is shown in Fig. 3.

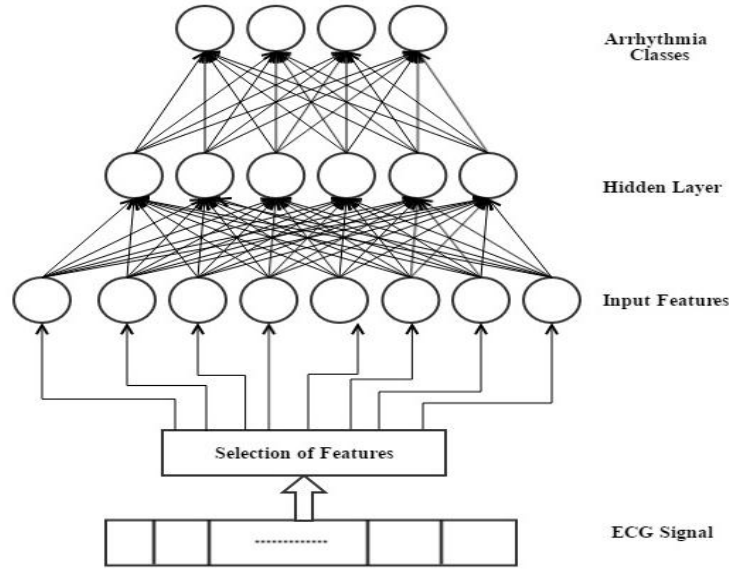


Fig. 3. Architecture of MLP neural network

2.5.2. Support Vector Machine (SVM)

SVM is a highly non-linear network structure works on structural risk minimization principle to classify correctly the unseen patterns [33]. It minimizing the training set error and maximizing the margin, with the aim of accomplishing the most excellent generalization capacity and staying resilient to over fitting. In this study we used the quadratic SVM structure to classify the ECG beats.

Also, one key benefit of SVM is the usage of convex quadratic programming that results just in global minima therefore avoiding of being stuck in local minima. Assume that our training data have N pairs $(x_1, y_1), (x_2, y_2), \dots, (x_N, y_N)$ with $x_i \in \mathbb{R}^p$ and $y_i \in \{-1, 1\}$.

Let a hyper-plane be $\{x: f(x) = x^T \beta + \beta_0 = 0\}$, where β is a unit vector,

$$G(x) = \text{sign}[x^T \beta + \beta_0] \quad (9)$$

Function $f(x)$ results in the signed distance from a point x .

Automatic classification of ECG signal consists of different features relating to fiducial point intervals of ECG in one cardiac cycle. Features relating to heartbeat intervals and ECG morphology were also calculated separately for each heartbeat in the ECG signals. The features extracted for one cardiac cycle are shown in Table 1. The block diagram of the ECG classification techniques is shown in Fig.4. The proposed classification process consists of extracting temporal, R-R interval and morphological features after detecting R peaks from the

pre-processed ECG signal. The mixture of features is applied to NN classifier for classifying different conditions (Normal, LBBBs, RBBBs and Paced beats) of the heart disorders.

Table 1. Extracted Features

Group	Features
Temporal	R-R intervals
Heart beat features	Q, R, S and T amplitudes QRS duration (QRS on and QRS off)
Morphology	Q-T interval, S-T interval

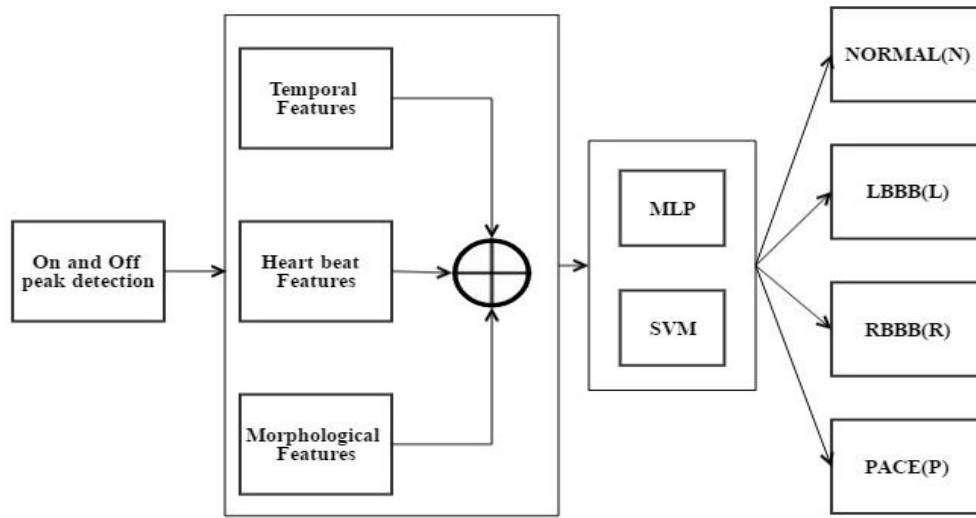


Fig. 4. Block diagram of ECG beat classification process

2.6. Performance measure

The performance of the proposed algorithm for QRS detection are evaluated for the sensitivity (Se), the positive predictivity (PP), classification accuracy (Acc) and the detection error rate (DER) using the following equations

$$Se = \frac{TP}{TP + FN} \times 100\%$$

$$PP = \frac{TP}{TP + FP} \times 100\%$$

$$DER = \frac{FP + FN}{TP} \times 100\%$$

The detection accuracy, the overall performance of the method is measured in terms of

$$Accuracy(Acc) = \frac{TP + TN}{TP + TN + FP + FN} \times 100\%$$

where TP=True positive is the correct detected R-peaks, FN=False negative is the undetected R-peaks, FP = False positive is the mis-detections, TN = Number of true negative beats

3. Results and discussion

The proposed R-peak detection and QRS complex method was evaluated using the MIT-BIH arrhythmia database. The recorded ECG signals are acceptable in quality, waves, QRS complex, and irregular heart rhythms. The performance of the proposed method is compared with some of the published results which are presented in Table 3.

3.1. R-peak detection

An abnormal ECG signal of record 117 is de-noised with wavelet transform and baseline wander correction is shown in Fig.5 to Fig.7. Fig. 8 shows the simulation results of R-peak detection in ECG recordings and the results of all 48 records of the MIT-BIH arrhythmia database are summarized in Table 2.

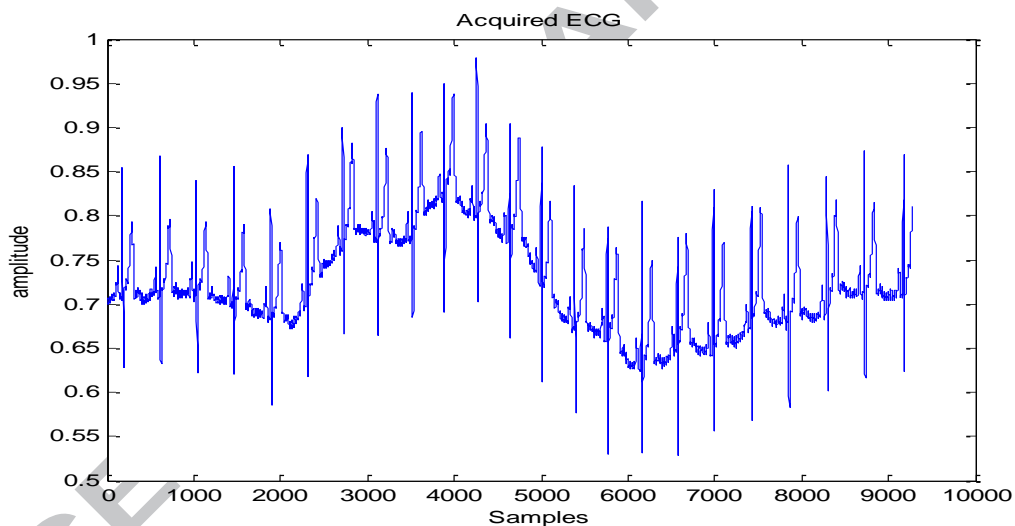


Fig.5. Original acquired ECG signal

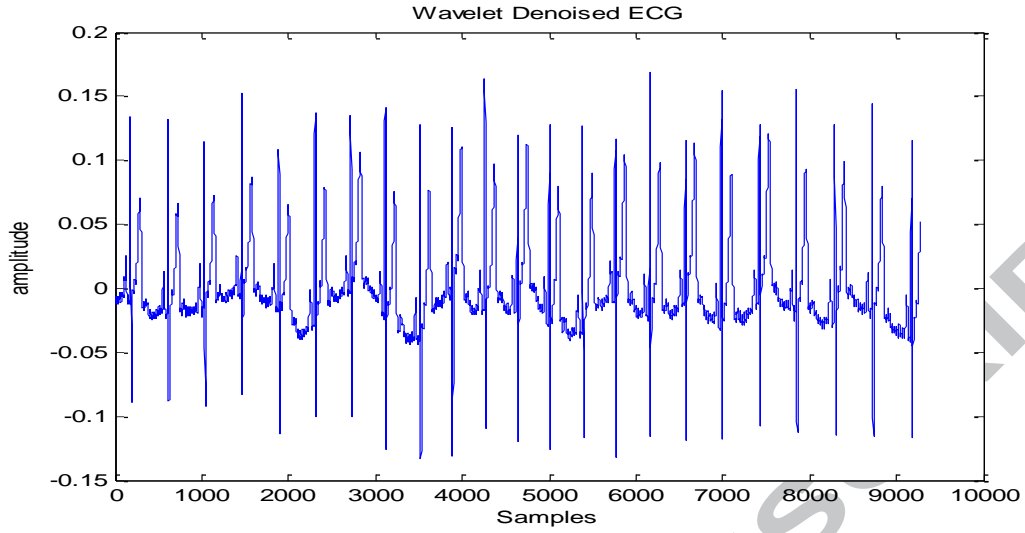


Fig.6. Wavelet de-noised ECG signal

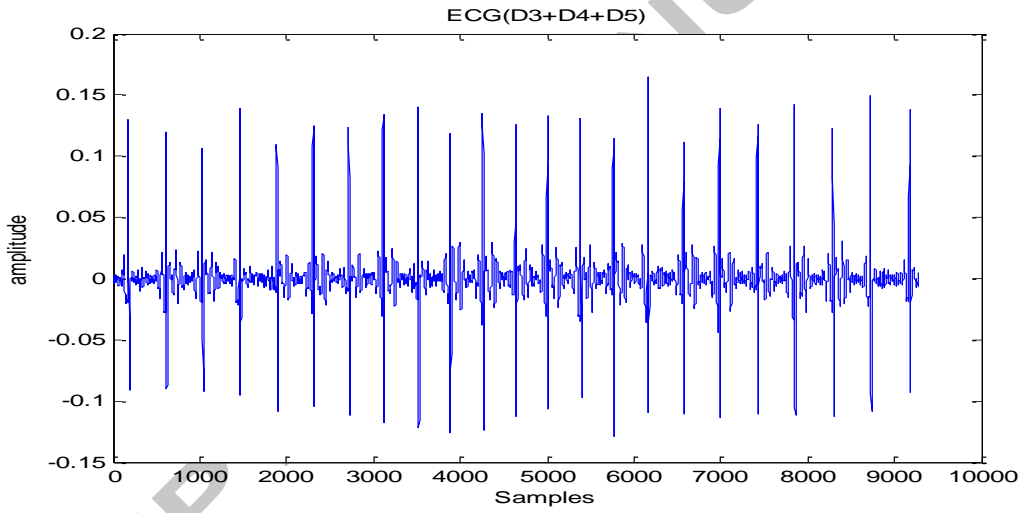


Fig. 7. Detection of (D3+D4+D5) selected ECG signal

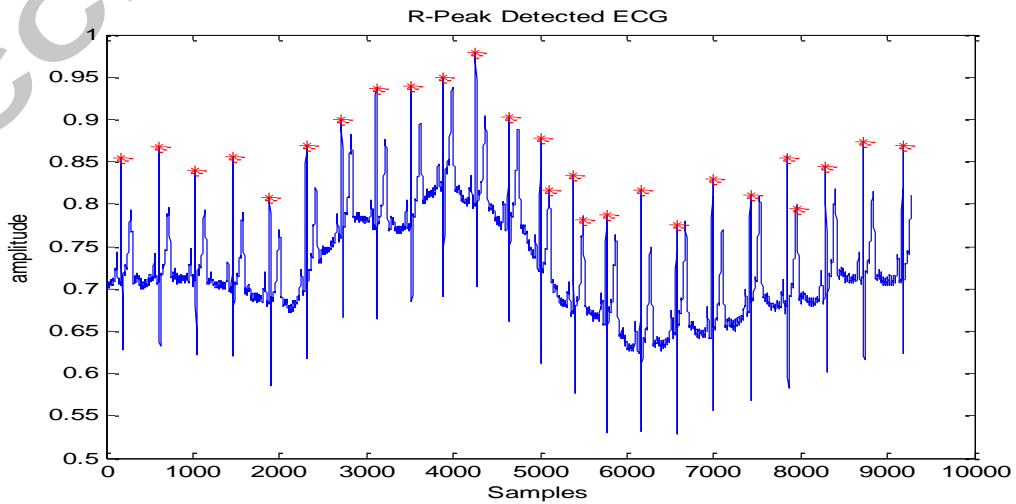


Fig. 8. R-peak detected ECG signal

3.2. QRS complex detection

In order to illustrate the ability of the proposed algorithm in detecting QRS complex with morphological features, the results of R-peak localisation in selected beats from ECG signal are presented. The selected beats contain different kinds of noise and cardiac anomalies. A normal ECG signal of record 103 from database is processed for noise elimination and is presented in Fig.9 to Fig. 11. The first segment presents a baseline drift, which is considered as a low-frequency noise. All the QRS complexes of the segmented signals are accurately detected, by correcting the baseline wander and de-noising the high-frequency noise in the pre-processing stage. The original noisy ECG is denoised shown with wavelet based decomposition and the selective coefficient of D3, D4, D5 of the signal is used for R-Peak detection. Fig. 12 represents the R-peaks detected signal. The obtained result shows the ability of the proposed multiresolution wavelet-based R-peak detection algorithm in presence of noise (high-frequency noise and baseline wander). The positive predictivity (PP) is used to discriminate between correct and false detections and the accuracy is tested by using the detection error rate (DER) as illustrated in Table 2 for all 48 records.

The proposed method detected 109666 beats (DB) from a total of 109494 annotation true beats (TB). It detected true positive of 109351, false-negative beats of 144, and false-positive beats for a total detection failure of 315 beats. The individual detection accuracies of the ECG records may vary from 98.99% to 100% depending on the characteristics of normal and pathological ECG signals and different noises. The obtained result shows the overall sensitivity (Se) of 99.87% and positive predictivity of 99.69%, respectively with an error rate for beat detection of 0.42% in detecting ECG beats. We observed high value error rate of 5.84% in the record 108 ECG data due to deformed morphologies of QRS complex. In order to assess the performance of proposed wavelet-based QRS detection algorithm, a comparative study is done with published results on the MIT-BIH database and summarised in Table 3. From the result, it is evident that the proposed algorithm provides a good accuracy with less error rate. Table 4 summarizes the comparison results of the minimum and maximum DER values of the proposed method with other published results.

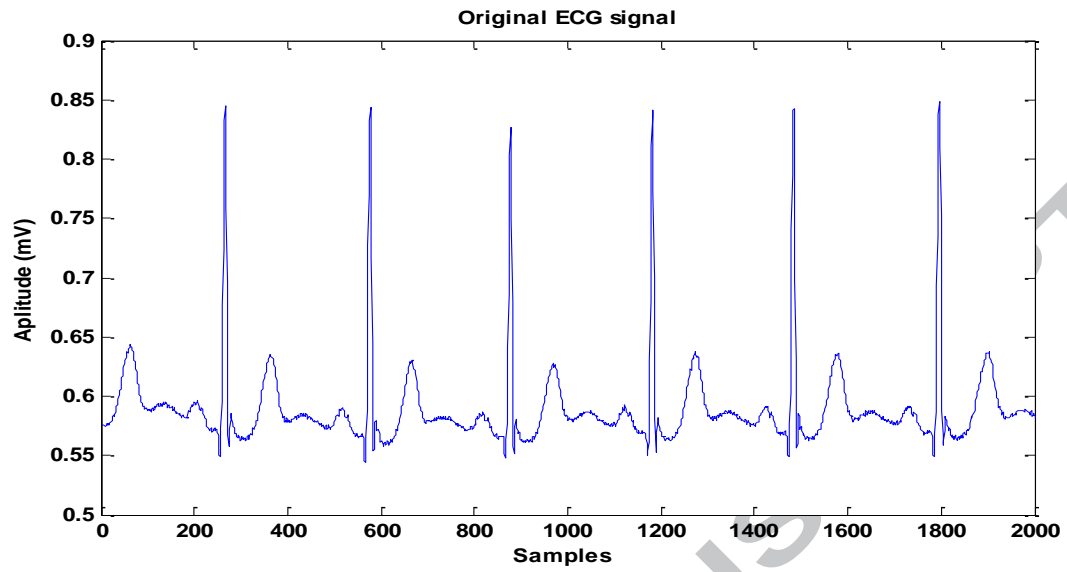


Fig.9. Original acquired normal ECG signal

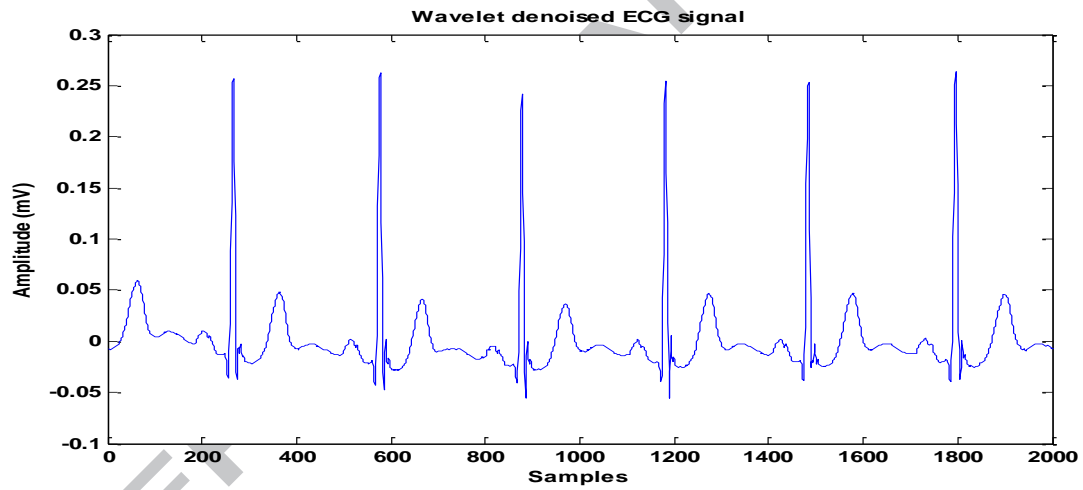


Fig.10. Wavelet denoised ECG signal

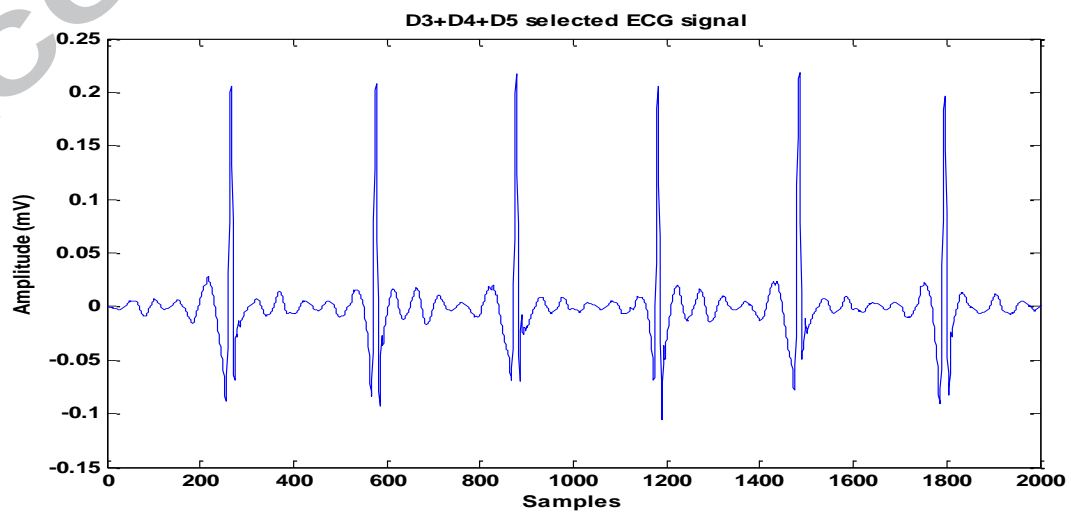
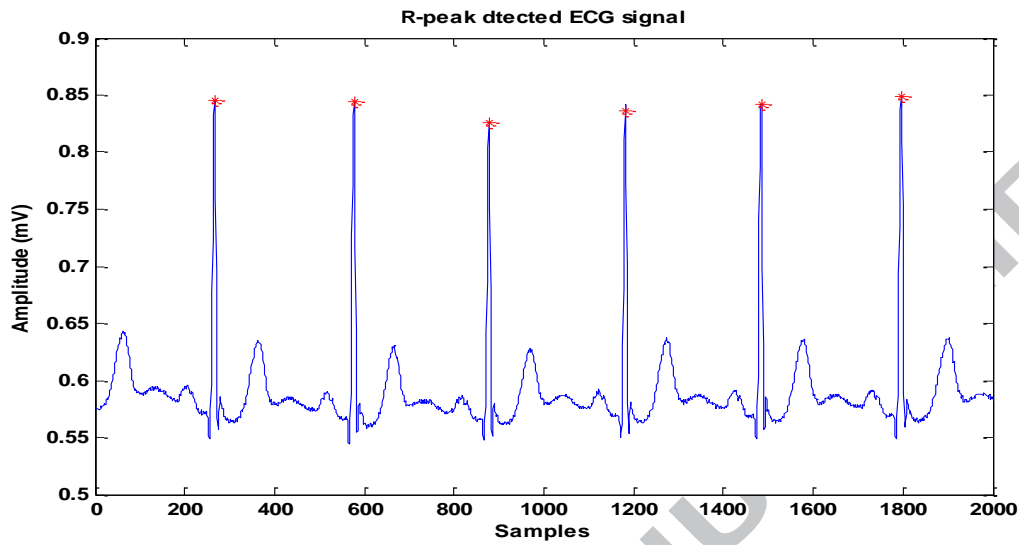


Fig. 11. Decomposed ECG signal (D3+D4+D5)**Fig 12.** R-peak detected ECG signal**Table 2.** Extracted parameter of the proposed method for ECG signals

Record No.	TB	DB	TP	FP	FN	Se%	PP%	DER%
100	2273	2273	2273	0	0	100	100	0
101	1865	1866	1863	3	2	99.89	99.83	0.26
102	2187	2187	2181	6	6	99.72	99.72	0.54
103	2084	2084	2084	0	0	100	100	0
104	2229	2260	2224	36	5	99.77	98.4	1.83
105	2572	2579	2569	10	3	99.88	99.61	0.5
106	2027	2025	2023	2	4	99.8	99.9	0.29
107	2137	2150	2134	16	3	99.85	99.25	0.88
108	1763	1850	1755	95	8	99.54	94.86	5.84
109	2532	2529	2528	1	4	99.84	99.96	0.19
111	2124	2124	2124	0	0	100	100	0
112	2539	2540	2539	1	0	100	99.96	0.03
113	1795	1796	1795	1	0	100	99.94	0.05
114	1879	1884	1879	5	0	100	99.73	0.26
115	1953	1953	1953	0	0	100	100	0
116	2412	2394	2391	3	21	99.12	99.87	0.99
117	1535	1540	1535	5	0	100	99.67	0.32
118	2278	2280	2278	2	0	100	99.91	0.08
119	1987	1988	1984	4	3	99.84	99.79	0.35
121	1863	1865	1862	3	1	99.94	99.83	0.21
122	2476	2476	2476	0	0	100	100	0
123	1518	1518	1518	0	0	100	100	0
124	1619	1619	1618	1	1	99.93	99.93	0.12
200	2601	2605	2601	4	0	100	99.84	0.15

201	1963	1964	1960	4	3	99.84	99.79	0.35
202	2136	2133	2133	0	3	99.85	100	0.14
203	2980	2984	2964	20	16	99.46	99.32	1.2
205	2656	2649	2644	5	12	99.54	99.81	0.64
207	1860	1865	1857	8	3	99.83	99.57	0.59
208	2955	2960	2952	8	3	99.89	99.72	0.37
209	3005	3026	3001	25	4	99.86	99.17	0.96
210	2650	2653	2644	9	6	99.77	99.66	0.57
212	2748	2751	2749	2	0	100	99.92	0.07
213	3251	3251	3251	0	0	100	100	0
214	2262	2257	2254	3	8	99.64	99.86	0.48
215	3363	3362	3355	7	8	99.76	99.79	0.44
217	2208	2212	2206	6	2	99.9	99.72	0.36
219	2154	2153	2152	1	2	99.9	99.95	0.13
220	2048	2048	2048	0	0	100	100	0
221	2427	2426	2425	1	2	99.91	99.95	0.12
222	2483	2481	2480	1	3	99.87	99.95	0.16
223	2605	2606	2605	1	0	100	99.96	0.03
228	2053	2060	2052	8	1	99.95	99.61	0.43
230	2256	2256	2256	0	0	100	100	0
231	1571	1571	1571	0	0	100	100	0
232	1780	1783	1780	3	0	100	99.83	0.16
233	3079	3077	3072	5	7	99.77	99.83	0.38
234	2753	2753	2753	0	0	100	100	0
Total	109494	109666	109351	315	144	99.873	99.696	0.4268

Table 3. Comparison of proposed method with published results for ECG signals analysis

QRS detection algorithm	NDB	TP	FP	FN	Se(%)	Pp(%)	DER (%)
Proposed Method	109666	110351	315	144	99.87	99.69	0.42
Pan et al.[23]	109809	109532	507	277	99.75	99.54	0.71
Banerjee et al.[31]	19098	19022	76	40	99.6	99.5	0.61
Bouaziz et al.[32]	109586	109354	232	140	99.87	99.79	0.34
Hamilton & Tompkins [34]	109267	108927	248	340	99.69	99.77	0.54
Zidelmal et al.[35]	109494	109101	193	393	99.64	99.82	0.54
Afonso et al.[36]	90909	90535	406	374	99.59	99.56	0.86
Arzeno et al.[37]	109456	107344	884	2112	98.07	99.59	2.79
Choi et al. 2010 [38]	109336	109,118	218	376	99.66	99.80	0.54
Chen et al.[39]	102654	102195	459	529	99.55	99.49	0.98

Karimipour et al. [40] 116253 115,945 308 192 99.81 99.70 0.49

Table 4. Comparison of DER values of proposed algorithm with published results

Rec. No. Methods	105	108	111	122	200	203	207	208	213	220	228	234
Proposed method	0.5	5.8	0	0	0.15	1.2	0.59	0.37	0	0	0.43	0
Pan et al. [23]	3.49	12.7	0.04	0.08	0.35	2.78	0.43	0.60	0.09	0	1.46	0
Banerjee et al.[31]	0.96	0	NA	NA	NA	NA	NA	NA	NA	NA	NA	NA
Bouaziz et al.[32]	0.81	8.4	0.09	0.04	0.3	1.24	0.64	0.08	0.03	0	0.73	0.04
Hamilton [34]	2.49	5.67	0.24	0	0.19	2.57	0.54	0.95	0.33	0	1.22	0
Zidelmali et al. [35]	2.29	3.4	0.09	0	1	2.05	1.08	1.02	0.03	0.05	4.09	0.33
Choi et al. [38]	2.02	4.71	0.09	0	1	2.05	1.18	1.02	0.03	0.05	3.56	0.04
Chen et al. [39]	3.22	NA	0.47	0	4.11	3.52	1.45	5.78	0.13	0	NA	0.11
Karimpour et al. [40]	2.41	12.9	0.04	0	0.19	3.63	0.37	0.23	0.03	0	1.12	0

3.3. Onset and Offset detection of ECG peaks

The complete QRS complex is detected by detecting R-peak with the Q and S points [31]. For Q-peak location (Qloc), 30 samples are searched at the left of fiducial point (Rloc); if a negative maximum is found at the left side of Rloc then Qloc is detected. Similarly 30 samples are chosen at the right side of the fiducial location to mark Sloc. The Q and S locations are stored in an array of Q-index and S-index and a search process is initiated by selecting 20 samples left of Qloc and right of Sloc, the minimum slope is marked as QRS_On and QRS_Off which is shown in Fig. 13 and Fig.14. For the T-peak localization, a window of Rloc+30 to Rloc+160 was chosen and the maximum value within the window is considered as Tloc. In a searching process, 30 and 50 samples are chosen at the left and right of Tloc, which are the standard samples of the normal T wave duration. The absolute minima in both sides of Tloc are measured as T_On and T_Off as shown in Fig.15.

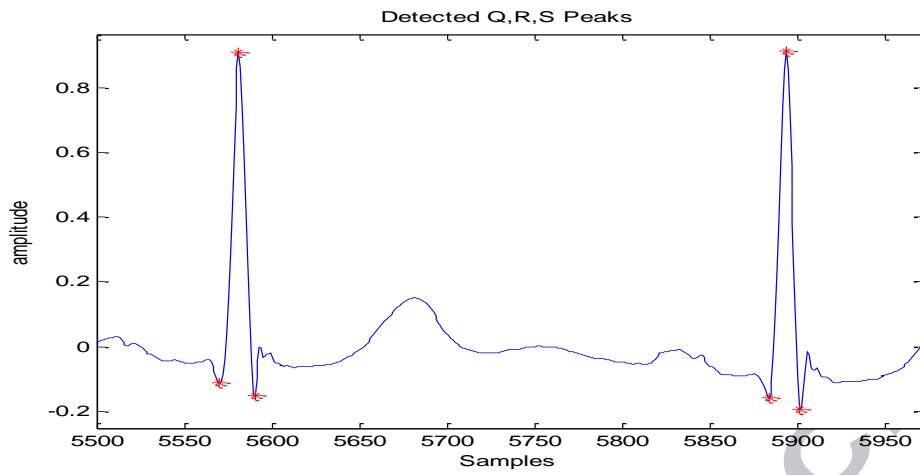


Fig. 13. Detected Q, R, S peaks

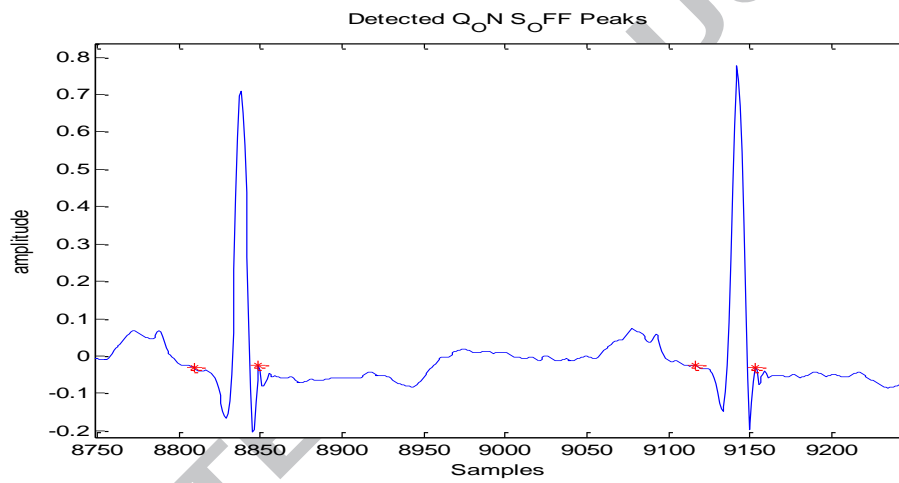


Fig. 14. Detected Q_{On} & S_{Off}

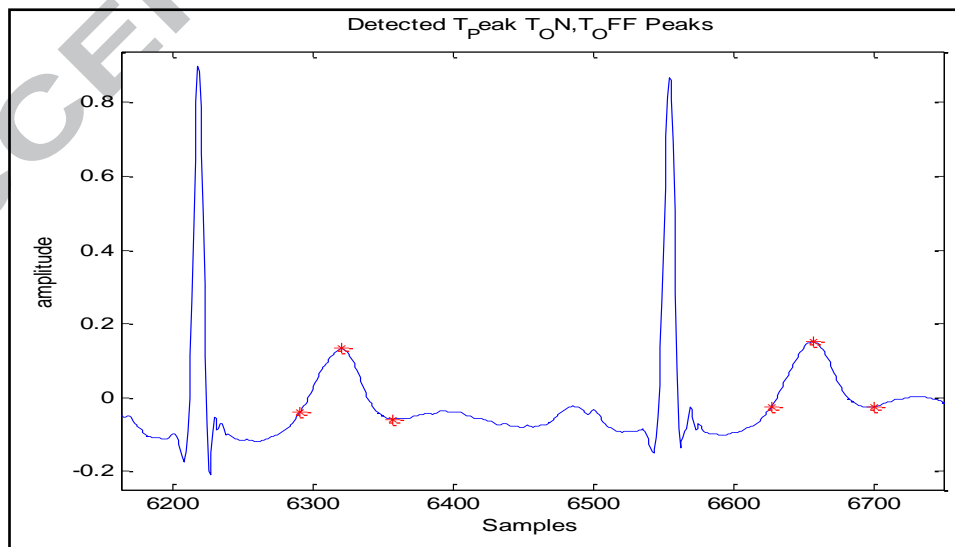


Fig. 15. Detected T_{on} , T_{off}

3.4. Extracted feature

A good feature extraction methodology would be helpful to classify the cardiac abnormalities accurately. The morphological features information of one cardiac cycle provides high classification accuracy for larger dataset. Using multiresolution wavelet transform, Q_Peak, R_Peak, S_Peak, T_Peak, QT_Interval, ST_Interval, RR_Interval and QRS duration features were extracted and the values are given in Table 5. The selected features were used for classification of cardiac conditions i.e. normal, LBBB, RBBB and paced beat in recorded ECG signals.

Table 5. Extracted features of ECG recorded signals

Record #	Qamp	Ramp	Samp	Tamp	QT_Int	ST_Int	RR_Int	QRS_Dur
100	-0.156	0.792	-0.151	0.025	0.389	0.464	0.813	0.105
101	-0.089	0.809	-0.094	0.096	0.324	0.334	0.845	0.176
102	-0.084	0.785	-0.192	0.115	0.355	0.363	0.826	0.165
103	-0.149	0.926	-0.161	0.157	0.299	0.351	0.855	0.089
104	-0.027	0.434	-0.180	0.103	0.411	0.437	0.801	0.130
105	-0.041	0.703	-0.133	0.065	0.322	0.327	0.723	0.168
106	-0.082	0.748	-0.152	0.152	0.311	0.345	0.886	0.165
107	-0.066	0.616	-0.669	0.367	0.381	0.366	0.850	0.222
108	-0.028	0.303	-0.069	0.061	0.415	0.395	0.662	0.167
109	-0.069	0.726	-0.3567	0.117	0.411	0.406	0.655	0.183
111	0.024	0.739	-0.294	0.257	0.311	0.329	0.849	0.145
112	-0.019	0.822	-0.305	0.153	0.382	0.422	0.701	0.156
113	-0.101	0.891	-0.205	0.381	0.357	0.434	1.016	0.118
114	-0.576	0.219	-0.704	0.363	0.291	0.368	0.985	0.120
115	-0.047	0.903	-0.378	0.063	0.395	0.430	0.959	0.107
116	-0.088	0.908	-0.181	0.157	0.283	0.313	0.761	0.144
117	-0.122	0.655	-0.784	0.562	0.347	0.397	1.202	0.170
118	-0.016	0.773	-0.623	0.076	0.398	0.395	0.828	0.176
119	0.003	0.637	-0.113	0.081	0.342	0.364	0.830	0.118
121	-0.041	0.789	-0.021	0.115	0.309	0.325	0.999	0.206
122	-0.192	0.9201	-0.127	-0.013	0.309	0.333	0.687	0.198
123	-0.045	0.866	-0.348	0.168	0.373	0.415	1.252	0.118
124	-0.041	0.896	-0.121	0.026	0.421	0.432	1.210	0.125
200	-0.028	0.399	-0.399	0.165	0.355	0.389	0.682	0.147
201	-0.041	0.866	-0.094	0.121	0.311	0.292	0.667	0.170
202	-0.001	0.838	-0.058	0.178	0.331	0.314	1.125	0.191
203	-0.044	0.622	-0.206	0.202	0.357	0.327	0.572	0.186
205	-0.119	0.899	-0.099	0.062	0.325	0.382	0.669	0.110
207	-0.072	0.227	-0.264	0.258	0.388	0.397	0.781	0.150
208	0.043	0.671	-0.144	0.124	0.373	0.374	0.574	0.145
209	-0.119	0.826	-0.499	0.151	0.251	0.317	0.642	0.114
210	-0.011	0.827	-0.154	0.052	0.412	0.369	0.661	0.156
212	-0.111	0.841	-0.374	0.251	0.289	0.296	0.659	0.211
213	-0.103	0.916	-0.362	0.241	0.281	0.333	0.542	0.113
214	-0.015	0.879	-0.087	0.018	0.409	0.362	0.796	0.148
215	-0.053	0.332	-0.262	0.156	0.235	0.288	0.536	0.136
217	-0.077	0.635	-0.849	0.448	0.385	0.396	0.821	0.195
219	0.001	0.925	-0.089	0.027	0.452	0.461	0.804	0.109
220	-0.043	0.892	-0.401	0.086	0.3411	0.355	0.834	0.139

221	-0.005	0.836	-0.136	0.110	0.363	0.380	0.763	0.118
222	-0.056	0.581	-0.103	0.036	0.234	0.296	0.801	0.092
223	0.003	0.899	-0.125	-0.005	0.403	0.419	0.749	0.111
228	-0.052	0.365	-0.054	0.08656	0.319	0.342	0.818	0.163
230	-0.031	0.686	-0.501	0.116	0.297	0.316	0.758	0.126
231	-0.202	0.825	-0.468	0.243	0.368	0.417	0.951	0.151
232	-0.057	0.705	-0.472	0.292	0.345	0.387	0.958	0.139
233	-0.017	0.672	-0.289	0.240	0.427	0.401	0.581	0.180
234	-0.071	0.834	-0.109	0.005	0.363	0.360	0.651	0.174

3.5. Classifier results

The input to the classifier is the set of features extracted from ECG signals representing different types of cardiac conditions. The data sets of different arrhythmia conditions of ECG signals have been considered for experimental analysis is given in Table 6. The feature data matrix [8×1071] is prepared by selecting 248, 296, 256 and 271 for Normal, LBBB, RBBB and Paced beats respectively and used as the input to the classifiers. The selected beats from feature set were randomly assigned into training and testing subset using ten-fold cross validation to train the classifiers. The simulation has been performed by using MLP-BP with learning rate 0.05 and SVM classifiers.

Table 7-8 summarizes the detail performance results in terms of sensitivity, specificity, and accuracy of the MLP-BP and SVM classifier at fold 7 and fold 6 respectively. The best validation performance confirms its superiority with an accuracy of 96.67% in MLP-BP at fold 7 and 98.39% in SVM at fold 6 respectively in detecting cardiac conditions is highlighted in Table 9. Thus the classification accuracy of the SVM approach proves superior to that of the NN classifier with extracted features. Fig. 16-18 shows the plot of sensitivity, specificity and classification accuracy using different classifiers for various folds in ten-fold cross validation.

Table 6. Distribution of ECG records for different conditions

Type	Records
Normal beat	100, 101, 103, 202, 205, 219, 230
LBBB beat	109, 111, 207, 214,
RBBB beat	118, 124, 212, 231
Paced beat	102, 104, 107, 217

Table 7. Classification result of MLP-BP at fold 7

Beat type	TP	FP	FN	TN	ACC	S _e	S _p	P	F-Score
N	241	7	24	760	96.99	97.17	96.93	90.94	93.95
LBBB	281	15	23	720	96.34	94.93	96.90	92.43	93.66
RBBB	251	5	5	750	99.01	98.04	99.33	98.04	98.04
Paced	228	43	17	773	94.34	84.13	97.84	93.06	88.37
	1001	70	69	3003	96.67	93.57	97.75	93.62	93.51

Table 8. Classification result of SVM at fold 6

Beat type	TP	FP	FN	TN	ACC	Se	Sp	P	F-Score
N	239	9	5	798	98.67	97.95	98.88	96.37	97.15
LBBB	286	10	8	751	98.29	97.28	98.69	96.62	96.95
RBBB	254	2	6	783	99.23	97.69	99.75	99.22	98.45
Paced	258	13	15	779	97.37	94.51	98.36	95.20	94.85
	1037	34	34	3111	98.39	96.86	98.92	96.85	96.85

Table 9. Performance analysis of the proposed method with the MLP and SVM classifier

Folds	MLP			SVM		
	Sensitivity (%)	Specificity (%)	Accuracy (%)	Sensitivity (%)	Specificity (%)	Accuracy (%)
2	87.55	95.37	93.28	96.82	98.69	98.22
3	89.75	96.23	94.49	96.72	98.88	98.34
4	86.47	95.25	92.83	96.30	98.72	98.10
5	87.81	95.46	93.46	96.05	98.66	98.01
6	91.09	96.92	95.26	96.86	98.92	98.39
7	93.57	97.76	96.67	95.80	98.56	97.86
8	89.67	96.40	94.45	96.19	98.69	98.06
9	89.69	96.22	94.52	95.99	98.62	97.96
10	90.11	96.50	94.76	96.45	98.79	98.20

The best performance results are indicated in bold.

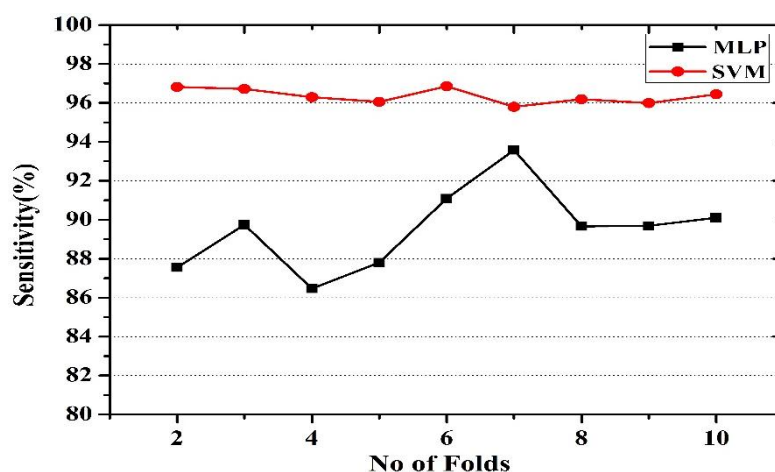


Fig. 16. Performance plot of ten-fold cross-validation versus sensitivity (%) for classifiers.

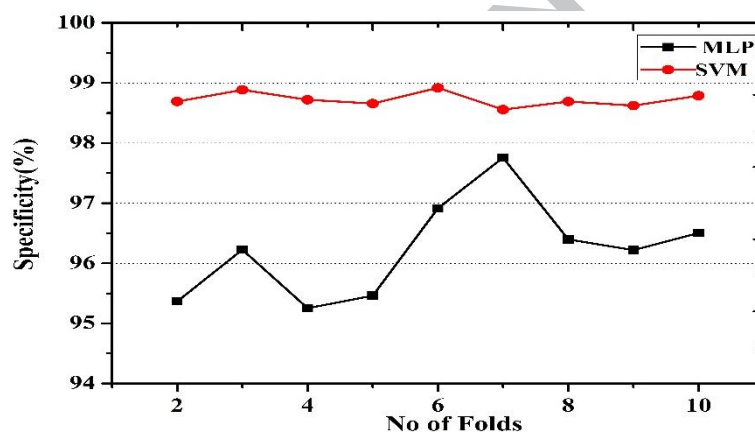


Fig. 17. Performance plot of ten-fold cross-validation versus specificity (%) for classifiers.

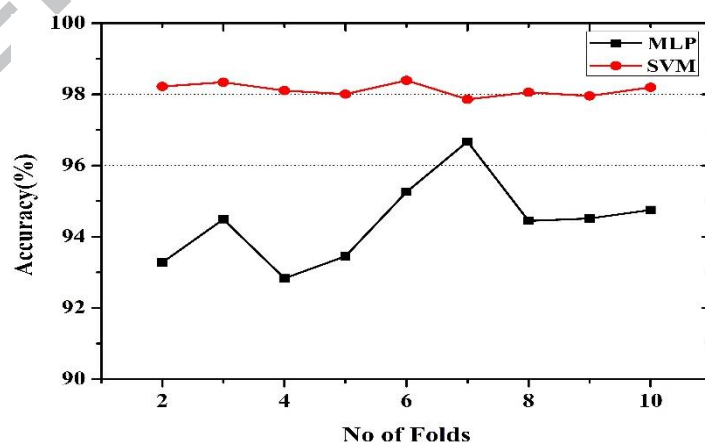


Fig. 18. Performance plot of ten-fold cross-validation versus accuracy (%) for classifiers.

4. Discussion

It is difficult to diagnose the arrhythmia condition due to presence of noise in ECG signal and irregularity in heartbeats. The computer-aided analysis assists the physicians for interpretation and detection of cardiac disorders. In this study, a modified approach has been proposed to detect the QRS complex based on wavelet transform and adaptive thresholding by identifying the complex onset and offset points. The extracted discriminant features were used to classify the types of ECG beats.

In this section, we compared the classification performance of our method with some of the published literature utilizing different features and classifiers. An innovative approach based on first-derivative and an adaptive threshold detected the onset and offset of QRS complex with sensitivity of 99.15% and the positive predictability of 99.18% in dataset [41]. Seven types of ECG beats were classified with accuracy of 96.06% in the fuzzy hybrid NN classifier using higher order spectra (HOS) features [42]. Martis et al. [43] obtained 94.52% using NN classifier in HOS cumulants features extracted with principal component analysis (PCA). The accuracy of 94.0% was obtained in classifying four types of ECG beats with the morphological and the inter-beat (RR) interval [44]. Similarly five classes of arrhythmia classified using DWT and dimensionality reduction methods with accuracy of 96.92% and 98.78% in SVM-RBF and NN respectively [45]. Ince et al. [46] obtained a classification accuracy of 95.58% in classify two types of class of arrhythmia in a PCA based feature extraction and optimized NN classifier. The bispectrum features extracted based on PCA based dimensionality reduction method achieved an accuracy of 93.48% with SVM classifier in classifying five types of beats. It [47]. In a recent work, an optimized block-based NN classified the arrhythmia with an accuracy of 97% in extracted Hermit function coefficient and temporal features from ECG signals [48]. The comparison of ECG beat classification accuracy of the proposed system and some existing systems are summarized in Table 10.

In this work, we have used multiresolution wavelet transform for de-noising and detecting QRS complex of ECG signal. The informative features has been extracted and classified for cardiac beats using MLP-BP and SVM classifier. The evaluated result shows the better detection performance with sensitivity of 99.87% and positive predictivity of 99.69% with less detection error rate of 0.42% in detecting QRS complex. The SVM classifiers confirmed its superiority in extracted features for classifying ECG beats with an accuracy of 98.39% compared to 96.67% in MLP-BP classifier. However, a recent work of automatic cardiac arrhythmia detection in ECG signal has been presented emphasizing the effectiveness of OPF classifier in terms of computation time, accuracy, sensitivity and specificity [50]. The effectiveness of OPF may be attributed to its characteristic of being

independent of hard-to-calibrate control parameter, and assumption of feature space, faster training and testing time, decisions based on global criteria.

Table 10. Classification performance of the proposed method and comparison with some existing method.

Literature	Features	Classifier	Classes	Accuracy (%)
Osowski & Linh [42]	HOS	Hybrid fuzzy NN	7	96.06%
Martis et al. [43]	Cumulant+PCA	NN	5	94.52%
Hu et al. [44]	Time domain features	Mixture of experts	2	94.00%
Martis et al. [45]	DWT+PCA	SVM-RBF	5	96.92%
Ince et al. [46]	DWT+PCA	MDPSO	5	95.58%
Martis et al. [47]	Bispectrum+PCA	SVM-RBF	5	93.48%
Shadmand and Mashoufi [48]	Hermit function coefficient and temporal features	Optimized block-based NN	5	97%
Proposed Methodology	DWT+ Temporal + Morphological	SVM	4	98.39%
		NN	4	96.67%

4. Conclusions

This paper presents a modified algorithm for accurate detection of QRS complex, extracting features based on the multiresolution wavelet transform and classifying for cardiac abnormalities using MLP-BP and SVM classifiers. The proposed method has shown better results in detecting QRS complex in terms of sensitivity and specificity with less detection error rate of 0.42% to detect cardiac abnormalities compared to existing published results. The classifiers confirmed the superiority of our proposed method in terms of higher accuracy for classifying four types of ECG beats: normal, LBBBs, RBBBs and Paced beat. The algorithm achieved average classification accuracy of 96.67% and 98.39% in MLP-BP and SVM classifiers respectively. The results suggests that the SVM classifier can have a significant role in interpretation of knowledge in diagnosis of cardiac abnormalities in the proposed method. We observed the SVM classifier is suitable for classifying ECG beats

using extracted features from the database. To perform real-time analysis of ECG signal where accuracy as well as computational time are most significant measures, more recent classifiers based on OPF may be focused for future work.

References

- [1] V.L. Roger, A.S. Go et al. Heart disease and stroke statistics-2012 update, *Circulation*. 125(1) (2012) e2–e220.
- [2] M.D. Huffman, D. Prabhakaran, Heart failure: epidemiology and prevention in India, *Natl. Med. J. India*. 23(5) (2010) 283-288.
- [3] A. Brenyo, K.A. Mehmet , Review of complementary and alternative medical treatment of arrhythmias, *The American journal of Cardiology* 113 (1) (2014) 897-903.
- [4] C. Martin, G. Matthews, C.L. Huang, Sudden cardiac death and inherited channelopathy: the basic electrophysiology of the myocyte and myocardium in ion channel disease, *Heart* 98 (2012) 536–543.
- [5] R. Mehra, Global public health problem of sudden cardiac death, *J. Electrocardiol.* 40 (6) (2007) S118-122.
- [6] C. Saritha, V. Sukanya, Y.N. Murthy, ECG signal analysis using wavelet transforms, *Bulg. J. Phys.* 35(2008) 68-77.
- [7] J.W. Magnini, E.Z. Gorodeski, et al., P wave duration is associated with cardiovascular and all-cause mortality outcomes: the National Health and Nutrition Examination Survey, *Heart Rhythm* 8 (1) (2011) 93-100.
- [8] H.M. Rai, A. Trivedi, S. Shukla, ECG signal processing for abnormalities detection using multiresolution wavelet transform and artificial neural network classifier, *Measurement* 46 (9) (2013) 3238-3246.
- [9] F. Zhang, Y. Lian, QRS detection based on multi-scale mathematical morphology for wearable ECG devices in body area networks, *IEEE Trans. Biomed. Circuits Syst.* 3 (4) (2009) 220-228.
- [10] X. Hongyan, H. Minsong, A new QRS detection algorithm based on empirical mode decomposition, in: *Proc of 2nd Int. Conf. on Bioinformatics and Biomedical Eng.* (2008), 693-696.
- [11] V. Almenar, A. Albiol, A new adaptive scheme for ECG enhancement, *Signal Process* 75(3) (1999) 253-263.

- [12] A. Gotchev, N. Nikolaev, K. Egiastian, Improving the transform domain ECG denoising performance by applying inter beat and intra beat de-correlating transforms, in: Proc of IEEE Int. Symposium on Circuits and Systems 2 (2001) 17-20.
- [13] A. Momot, Methods of weighted averaging of ECG signals using Bayesian inference and criterion function minimization, Biomed. Signal Proc. Control 4(2) (2009) 162-169.
- [14] M.P.S. Chawla, H.K. Verma, V. Kumar, ECG modeling and QRS detection using principal component analysis, in: Proc of the IET 3rd Int. Conf. on Advances in Medical, Signal and Information Processing (2006) 1-4.
- [15] A.K. Barros, A. Mansour, N. Ohnishi, Removing artifacts from electrocardiographic signals using independent components analysis, Neurocomputing 22(1-3) (1998) 173-186.
- [16] J.C.T.B. Moraes, M.O. Seixas, F.N. Vilani, E.V. Costa, A real time QRS complex classification method using Mahalanobis distance, Comput. Cardiol. (2002) 201-204.
- [17] K. Minami, H. Nakajima, T. Toyoshima, Real-time discrimination of ventricular tachyarrhythmia with Fourier-transform neural network, IEEE Trans. Biomed. Eng. 46(2) (1999) 179-185.
- [18] S. Osowski, T.H. Linh, ECG beat recognition using fuzzy hybrid neural network, IEEE Trans. Biomed. Eng. 48(11) (2001) 1265-1271.
- [19] O. Pahlm, L. Sornmo, Software QRS detection in ambulatory monitoring - a review, Med. Biol. Eng. Comput. 22 (4) (1984) 289-297.
- [20] B.U. Kohler, C. Hennig, R. Orglmeister, The principles of software QRS detection, IEEE Eng. Med. Biol. Mag. 21(1) (2002) 42-57.
- [21] A. Illanes-Manriquez, Q. Zhang, An algorithm for robust detection of QRS onset and offset in ECG signals, Computers in Cardiology 35 (2008) 857-60.
- [22] A. Martinez, R. Alcaraz, J.J. Rieta, Application of the phasor transforms for automatic delineation of single-lead ECG fiducial points, Physiol. Meas. 31(11) (2010) 1467-85.
- [23] J. Pan, W.J. Tompkins, A real-time QRS detection algorithm, IEEE Trans. Biomed. Eng. 32(3) (1985) 230-236.
- [24] S. Suppappola, Y. Sun, Nonlinear transform of ECG signals for digital QRS detection: a quantitative analysis, IEEE Trans. Biomed. Eng. 41(4) (1994) 397-400.
- [25] P.S. Addison, J.N. Watson, G.R. Clegg, M. Holzer, F. Sterz, C.E. Robertson, Evaluating arrhythmias in ECG signals using wavelet transforms, IEEE Eng. Med. Biol. 19(5)(2000) 104-109.

- [26] A.S. Al-Fahoum, I. Howitt, Combined wavelet transformation and radial basis neural networks for classifying life-threatening cardiac arrhythmias, *Med. Biol. Eng. Comput.* 37(5) (1999) 566-573.
- [27] C. Li, C. Zheng, C. Tai. Detection of ECG characteristic points using wavelet transforms, *IEEE Trans Biomed Eng.* 42 (1) (1995) 21-28.
- [28] J.P. Martinez, R. Almeida, S. Olmos, A.P. Rocha, P. Laguna, A wavelet based ECG delineator: evaluation on standard database, *IEEE Trans. Biomed. Eng.* 51(4) (2004) 570-581.
- [29] S. Pal, M. Mitra, Detection of ECG characteristic points using multiresolution wavelet analysis based selective coefficient method, *Measurement* 43(2) (2010) 255-261
- [30] A. Ghaffari, H. Golbayani, M. Ghasemi, A new mathematical based QRS detector using continuous wavelet transform, *Computers and Electrical Engineering* 34(2) (2008) 81-91.
- [31] S. Banerjee, R. Gupta, M. Mitra, Delineation of ECG characteristic features using multiresolution wavelet analysis method, *Measurement* 45(3) (2012) 474-487
- [32] F. Bouaziz, D. Boutana, M. Benidir, Multiresolution wavelet-based QRS complex detection algorithm suited to several abnormal morphologies, *IET Signal Processing* 8(7) (2014) 774-782.
- [33] N. Cristianini, J. S. Taylor, An introduction to support vector machines and other kernel based learning methods, Cambridge University Press (2000).
- [34] P.S. Hamilton, W.J. Tompkins, Quantitative investigation of QRS detection rules using the MIT/BIH arrhythmia database, *IEEE Trans. Biomed. Eng.* 33(12) (1986) 1157-1165.
- [35] Z. Zidmal, A. Amirou, M. Adnane, A. Belouchrani, QRS detection based on wavelet coefficients, *Comput. Methods Programs Biomed.* 107(3) (2012) 490-496.
- [36] V.X. Afonso, W.J. Tompkins, T.Q. Nguyen, S. Luo, ECG beat detection using filter banks, *IEEE Trans. Biomed. Eng.* 46(2) (1999) 192-201.
- [37] N.M. Arzeno, Z.D. Deng, C.S. Poon, Analysis of first derivative based QRS detection algorithm, *IEEE Trans. Biomed. Eng.* 55(2) (2008) 478-484.
- [38] S. Choi, M. Adnane, G.J. Lee, H. Jang, Z. Jiang, H.K. Park, Development of ECG beat segmentation method by combining lowpass filter and irregular R-R interval checkup strategy, *Expert Systems with Applications* 37(7) (2010) 5208-5218.
- [39] S.W. Chen, H.C. Chen, H.L. Chan, A real-time QRS method based on moving-averaging incorporating with wavelet denoising, *Comput. Method Programs Biomed.* 82(3) (2006) 187-195.

- [40] A. Karimipour, M.R. Homaeinezhad, Real-time electro cardiogram P-QRS-T detection–delineation algorithm based on quality-supported analysis of characteristic templates, *Comput. Biol. Med.* 52 (2014)153-165.
- [41] P.V.M. Joao, C.C. Paulo, A.L.M. Joao, R.V.S. Carlos, R.M. Carlos, An innovative approach of QRS segmentation based on first-derivative, Hilbert and Wavelet Transforms, *Medical Engineering & Physics* 34(9) (2012) 1236-1246.
- [42] S. Osowski, T.H. Linh ECG beat recognition using fuzzy hybrid neural network, *IEEE Trans. Biomed. Eng.* 48 (11) (2001) 1265-1271.
- [43] R.J. Martis, U.R. Acharya, C.M. Lim, K. Mandana, A.K. Ray, C. Chakraborty Application of higher order cumulant features for cardiac health diagnosis using ECG signals *Int. J. Neural Syst.*, 23 (04) (2013).
- [44] Y.H. Hu, S. Palreddy, W.J. Tompkins, A patient-adaptable ECG beat classifier using a mixture of experts approach, *IEEE Trans., Biomed. Eng.* 44 (9) (1997) 891-900.
- [45] R.J. Martis, U.R. Acharya, L.C. Min ECG beat classification using PCA, LDA, ICA and discrete wavelet transform, *Biomed. Signal Process. Control*, 8 (5) (2013) 437-448.
- [46] Ince, S. Kiranyaz, M. Gabbouj A generic and robust system for automated patient-specific classification of ECG signals, *IEEE Trans. Biomed. Eng.* 56 (5) (2009) 1415-1426.
- [47] R.J. Martis, U.R. Acharya, K. Mandana, A. Ray, C. Chakraborty Cardiac decision making using higher order spectra, *Biomed. Signal Process. Control*, 8 (2) (2013), 193-203.
- [48] S. Shadmand, B. Mashouf, A new personalized ECG signal classification algorithm using block-based neural network and particle swarm optimization, *Biomed. Signal Process. Control*. 25 (2016) 12-23.
- [49] E.J da S. Luz, T.M. Nunes, V.H.C. de Albuquerque, J.P. Papa, D. Menotti, ECG arrhythmia classification based on optimum-path forest, *Expert Syst Appl.* 40 (2013) 3561-3573.
- [50] V.H.C. de Albuquerque, T.M. Nunes, D. R. Pereira, E.J. da S. Luz, D. Menotti, J.P. Papa, J.M.R. S. Tavares, Robust automated cardiac arrhythmia detection in ECG beat signals, *Neural Comput & Applic*, (2016) 1-15.

- De-noising and detection of QRS complex of ECG signals using wavelet transform.
- Extraction of informative features Classification of ECG beats using neural network and SVM classifier.
- Comparison and discussion of results.

ACCEPTED MANUSCRIPT